Electronic Supplementary Material (ESI) for Soft Matter.

Supporting Information

Hierarchical Self-Assembly of Metal-Organic Supramolecular Fibers with Lanthanide-derived Functionalities

Bohang Wu,[a] Yutao Tong,[a] Jiahua Wang,[a] Yuening Qiu,[a] Yifan Gao,[a] Martien A. Cohen Stuart,[a] Junyou Wang[a,*]

[a] East China University of Science and Technology, Department of Chemical Engineering, Meilong Road 130, 200237 Shanghai, China.

* Correspondence to: junyouwang@ecust.edu.cn

Content

1. Materials and methods

Materials and instruments

Europium(III) nitrate hexahydrate ($Eu(NO_3)_3 \cdot 6H_2O$), lanthanum(III) nitrate hexahydrate ($La(NO_3)_3 \cdot 6H_2O$), terbium(III) nitrate hexahydrate ($Tb(NO_3)_3 \cdot 6H_2O$), gadolinium(III) chloride hexahydrate ($GdCl_3 \cdot 6H_2O$), urea, tetrahydrofuran (THF) and D_2O were obtained from Sigma Aldrich and used without further purification. THF-D8 was obtained from TCI and used without further purification.

DPA molecule, ligand L_3 and BL_3 were synthesized according to literature.[1,2]

Light scattering (LS)

Light scattering (LS) measurements were performed with an ALV light scattering apparatus, equipped with a 21 mW He-Ne laser operating at a wavelength of 632.8 nm. Measurements were done at a detection angle of 90° unless stated otherwise. All measurements were performed at room temperature.

For angular-dependent LS, ten correlation functions $g_2(t)$ were recorded at 5 angles θ, from 30 to 110° in increments of 20°, to evaluate the angular dependence of the diffusion coefficient D.[3] It is known that asymmetric particles always give rise to a dependence of D (= Γ/q^2) on q^2, but for spherical particles, the D values should be independent of the scattering vector, because of the undetectable rotational motion. q is the scattering vector:

$$q = \frac{4\pi n}{\lambda} * \sin\frac{\theta}{2} \qquad \text{Equation S1}$$

Herein, n is the refractive index of the solvent, and λ is the wavelength of incident light.

Fluorescence spectroscopy

Solution of supramolecular fibers was put in 1.0 cm quartz cells for steady state and lifetime measurements on a Cary-4000 spectrometer. The slit was set at 5 nm and the spectra were corrected for the instrumental function. The excitation is set at 292 nm, and the emission spectra was recorded in the range of 450 - 750 nm.

To calculate the $q_{average}$, the exponential function (Expdec1) was applied to fit the datapoints. The k_{H2O} and k_{D2O} (represent the rate constants of luminescence decay) can be estimated from fitting table. The $q_{average}$ can be calculated based on Equation S2.[3]

$$q = 1.2 * (k_{H2O} - k_{D2O} - 0.25) \qquad \text{Equation S2}$$

X-ray diffraction (XRD)

X-ray diffraction (XRD) patterns of the samples were measured on a 18KW/D/max2550VB/PC powder diffraction system operated at 40 kV and 100 mA using Cu Kα radiation (λ = 1.542 Å), and a scan rate of 5° min^{-1} was applied to record the patterns in the range of 10° to 90°.

Transmission electron microscopy (TEM) and field emission scanning electron microscope (FE-SEM)

TEM was performed on a JEM-1400 electron microscope operating at 100 kV. 230-mesh copper grids were coated with formvar support film, followed by subsequent coating with carbon.

FE-SEM was performed on a Nova NanoSEM 450.

MRI testing and T_1 relaxation time

The MRI tests and T_1 relaxation time measurements were carried out on a 0.47 T NMRI20-Analyst NMR Analyzing and Imaging system (Niumag Corporation, Shanghai, China).

2. Sample preparation

Preparation of lanthanide-based supramolecular fiber

For a 1 mL sample (M/L = 1/1), THF (500 μL) and H_2O (380 μL) were first mixed, then an aqueous stock solution (L_3 molar concentration is 1 mM) of the L_3 (100 μL) was added under shaking, finally an aqueous stock solution (5 mM) of lanthanide metal ions (20 μL) was added under shaking. The final concentration of L_3 is 0.1 mM. The volume ratio of THF and H_2O was kept at v/v = 50/50. All stock solutions of L_3 and lanthanide ions were separately prepared in DI water.

For other samples with different M/L ratio, we can prepare these samples by simply tuning the volume of lanthanide ions stock solution. The volume ratio of THF and H_2O was kept at v/v = 50/50.

For the samples prepared in D_2O and THF-D8, all stock solutions were prepared in D_2O. THF-D8 (500 μL) and D_2O (380 μL) were first mixed, followed by addition of 100 μL L_3 stock solution (1 mM) and 20 μL europium ions Eu^{3+} stock solution (5 mM).

Transmission electron microscopy (TEM) and field emission scanning electron microscope (FE-SEM) measurements

For TEM measurements, 15 μL of the sample solution was placed on the 230-mesh copper grids. Excess solution was removed by filter paper, and samples were allowed to dry in ambient air at room temperature before TEM observation.

For SEM measurements, the precipitate was placed on the test platform for SEM observation.

Powder X-ray diffraction (XRD) measurements

For XRD measurements, 100 mL Eu^{3+}-L_3 samples (precipitate sample and fiber

sample) were prepared as above. For precipitate sample, the insoluble precipitate can be easily separated by centrifugation (14000 rpm, 15 min). For fiber sample, the excess solvent can be removed by freeze-drying, then the fiber powder was obtained for XRD measurements.

Fluorescence test

For fluorescence measurements, we firstly prepared 0.1 mM Eu^{3+}/Tb^{3+}-L_3 fiber as above procedure. We kept the total concentration of lanthanide ions as 0.1 mM in samples. For example, for a Eu^{3+}/Tb^{3+} mixed sample (Eu^{3+}% = 60%, namely Eu^{3+}/Tb^{3+} = 1/1), the Eu^{3+} and Tb^{3+} concentration in solution is 0.06 mM and 0.04 mM, respectively. Similarly, 0.1 mM Eu^{3+}-DPA assemblies was also prepared as above procedure.

MRI test and T_1 relaxation time

For MRI measurements, we firstly prepared 0.1 mM $Eu^{3+}/Tb^{3+}/Gd^{3+}$-L_3 fiber as above procedure (Herein, the concentration for Gd^{3+} (or Eu^{3+} or Tb^{3+}) is 0.0333 mM). To prepare 0.08 mM $Eu^{3+}/Tb^{3+}/Gd^{3+}$-L_3 fiber, we mixed 800 μL of 0.1 mM $Eu^{3+}/Tb^{3+}/Gd^{3+}$-L_3 solution and 200 μL THF/H_2O (v/v = 50/50) together (The concentration for Gd^{3+} (or Eu^{3+} or Tb^{3+}) is 0.0267 mM). For 0.06 mM $Eu^{3+}/Tb^{3+}/Gd^{3+}$-L_3 fiber, the concentration for Gd^{3+} (or Eu^{3+} or Tb^{3+}) is 0.02 mM. For 0.04 mM $Eu^{3+}/Tb^{3+}/Gd^{3+}$-L_3 fiber, the concentration for Gd^{3+} (or Eu^{3+} or Tb^{3+}) is 0.0133 mM. For 0.02 mM $Eu^{3+}/Tb^{3+}/Gd^{3+}$-L_3 fiber, the concentration for Gd^{3+} (or Eu^{3+} or Tb^{3+}) is 0.0067 mM.

3. Luminescence excitation of Eu^{3+}-L_3 assemblies

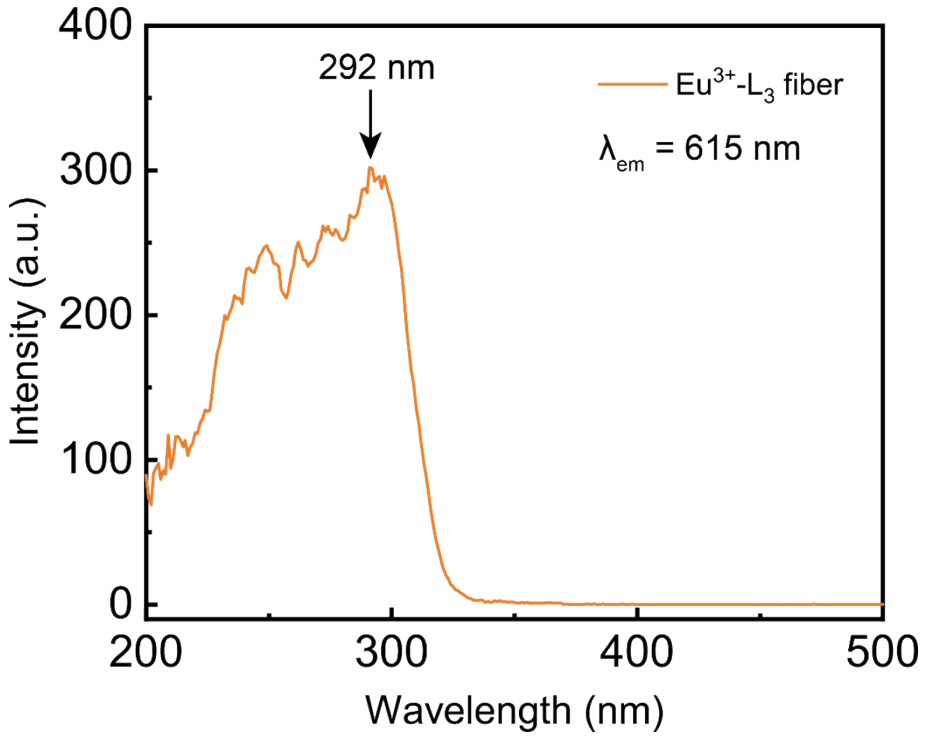

Figure S1. Luminescence excitation spectra of Eu^{3+}-L_3 assemblies taken at emission wavelength λ_{em} = 615 nm.

4. Samples with different Eu^{3+}/L_3 ratio

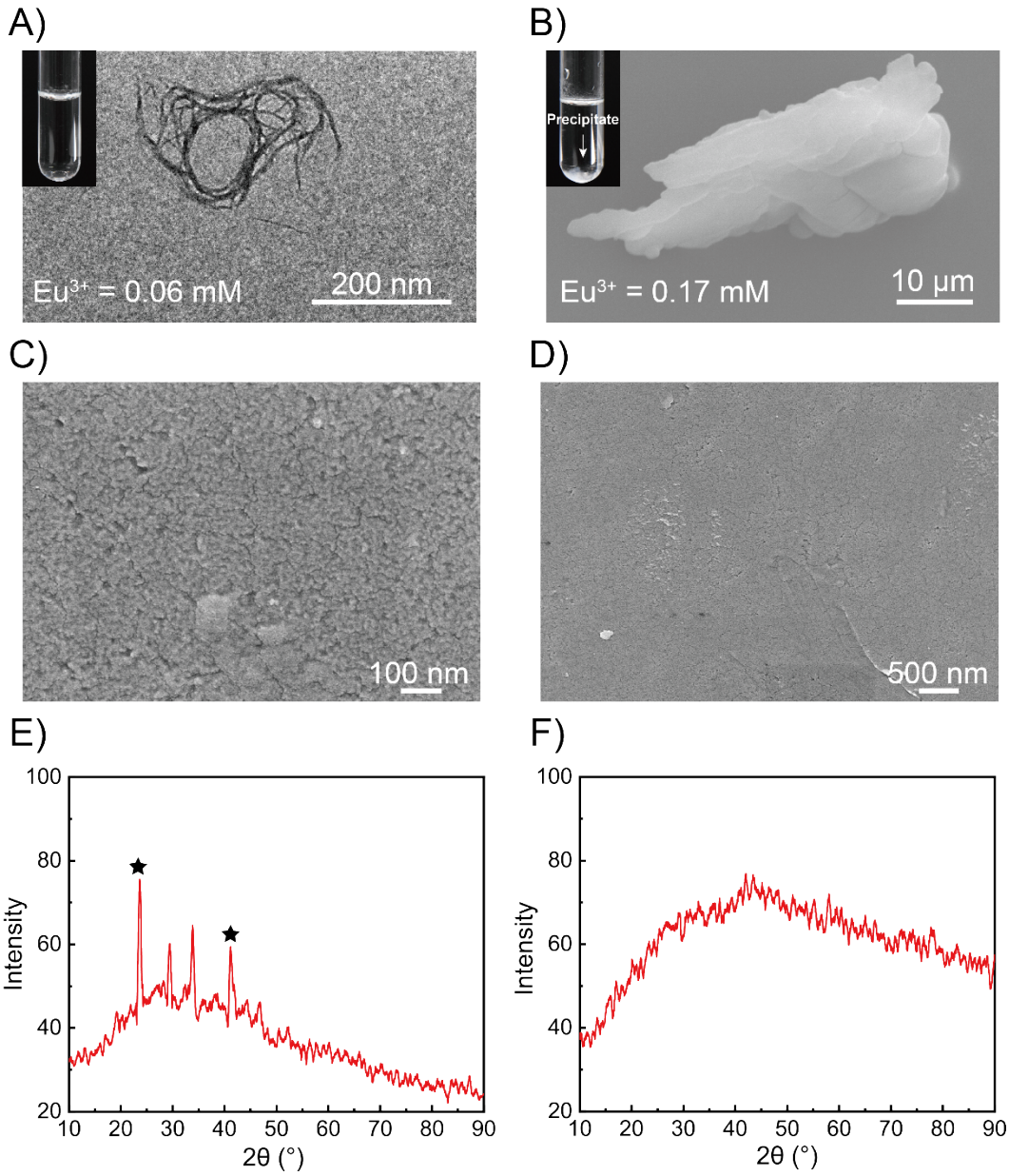

Figure S2. A) TEM images of Eu^{3+}-L_3 fiber: at Eu^{3+} = 0.06 mM. B), C) and D) SEM images of Eu^{3+}-L_3 precipitate: at Eu^{3+} = 0.17 mM (at different magnifications). XRD data of Eu^{3+}-L_3 fiber (Eu^{3+} = 0.1 mM) and F) Eu^{3+}-L_3 precipitate (Eu^{3+} = 0.17 mM). The distance of stacked monomer units can be calculated by the peaks marked by asterisk.

As shown in Figure S2E, four peaks can be observed at 22°, 27°, 34° and 44°, respectively (2θ, from left to right). Thus, the corresponding θ values are 11.0°, 13.5°, 17.0° and 22.0°, respectively (2θ, from left to right). We first assign the main peaks, marked with an asterisk. Using Bragg's Law ($d = n\lambda / 2\sin\theta$, λ = 1.542 Å), the d for θ = 11.0° can be calculated as 4.0 Å (n = 1), which is quite comparable to the typical inter-BTA-ring stacking distance (3.8 Å).[4] The peak with θ = 22.0° can also be assigned to the stacking distance, giving d = 4.1 Å (n = 2). Since the reflection intensity gradually attenuates, the higher order peaks (n = 3, 4, 5…) are unobservable.

So the main conclusion is that the fibrillar sample has a periodic structure, as expected for a stacked object, whereas the amorphous precipitate has not (Figure S2F).

One may wonder what the other (weak) peaks (θ= 13.5° and 17.0°, no asterisk) represent. Clearly, they do not come from the main fibrous component, but possibly from minority components with slightly different structures. We propose two possible structures. With the evaporation of solvent, individual fibers may be pushed together; where they touch, sections of interdigitating clusters may form, which have a smaller stacking distance. Moreover, some thin fibers (around 2 nm diameter), consisting of single-BTA stacks, may coexist with the main fiber component (12 nm), and thin fibers may have a smaller stacking distance that the main component. The 13.5° reflection would correspond to 3.3 Å, which is reminiscent of the distance quoted in reference.[4] We admit that these assignments are speculative, but it should be realized that the fact that both peaks are weak is in line with the assignment to a minority component. Moreover, 2 nm fibers would easily escape observation in TEM images, but could be picked by the XRD experiment.

5. Luminescence lifetime measurements

Table S1. Main model parameters for Eu^{3+}-L_3 fiber in H_2O and THF

Model	ExpDec1
Equation	$y = A_1 * \exp(-x/t_1) + y_0$
y_0	0.29158 ± 0.07286
A_1	327.13675 ± 0.85081
t_1	0.30429 ± 0.00113
τ	0.21092 ± 0.000779859
Adj. R-Square	0.9997

Table S2. Main model parameters for Eu^{3+}-L_3 fiber in D_2O and THF-D8

Model	ExpDec1
Equation	$y = A_1 * \exp(-x/t_1) + y_0$
y_0	4.56669 ± 0.72664
A_1	772.94639 ± 1.94398
t_1	1.81611 ± 0.00919
τ	1.25883 ± 0.00637
Adj. R-Square	0.99956

6. Molecular simulation

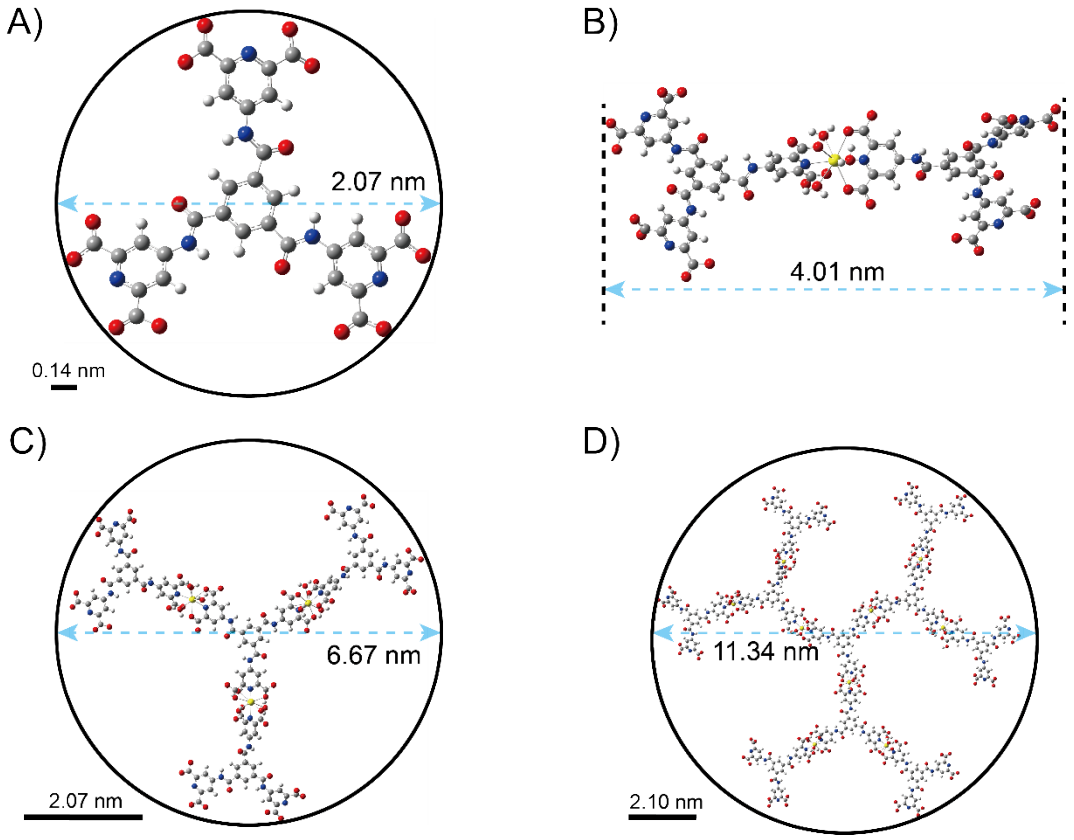

Figure S3. A) The single ligand, 2.07 nm. B) The Eu^{3+}-$(L_3)_2$ complex, 4.01 nm. C) The $Eu^{3+}{}_3$-$(L_3)_4$ complex, 6.67 nm. D) The $Eu^{3+}{}_9$-$(L_3)_{10}$ complex, 11.34 nm.

The L_3 itself and several metal-ligand clusters were studied by density functional theory (DFT), using the Gaussian 09 program package.[5] The structures were fully optimized by using B3LYP-D3 functions in combination with the def2-SVP basis and the SMD continuum solvent model.[6-9] The complexes $Eu^{3+}{}_3$-$(L_3)_4$ and $Eu^{3+}{}_9$-$(L_3)_{10}$ were optimized with GFN-XTB, followed by re-optimization using the Gaussian 09 program. The diameter was measured as that of the smallest circle in which the entire structure could be fitted. The results are shown in Figure S3.

For the single molecule L_3, its size is 2.07 nm; the end-to-end length of Eu^{3+}-$(L_3)_2$ is 4.01 nm; the diameter of $Eu^{3+}{}_3$-$(L_3)_4$ complex is 6.67 nm; the diameter of $Eu^{3+}{}_9$-$(L_3)_{10}$ complex is 11.34 nm.

By comparing to the experimentally found diameter of fibers (12 nm), we adopt $Eu^{3+}{}_9$-$(L_3)_{10}$ as the most representative subunit (containing 27 sites for combining H_2O molecules, which is consistent with the $q_{average}$). Note that the THF molecule is too large to fit the coordination site of lanthanide in the $Eu^{3+}{}_9$-$(L_3)_{10}$ cluster based on DFT simulation.

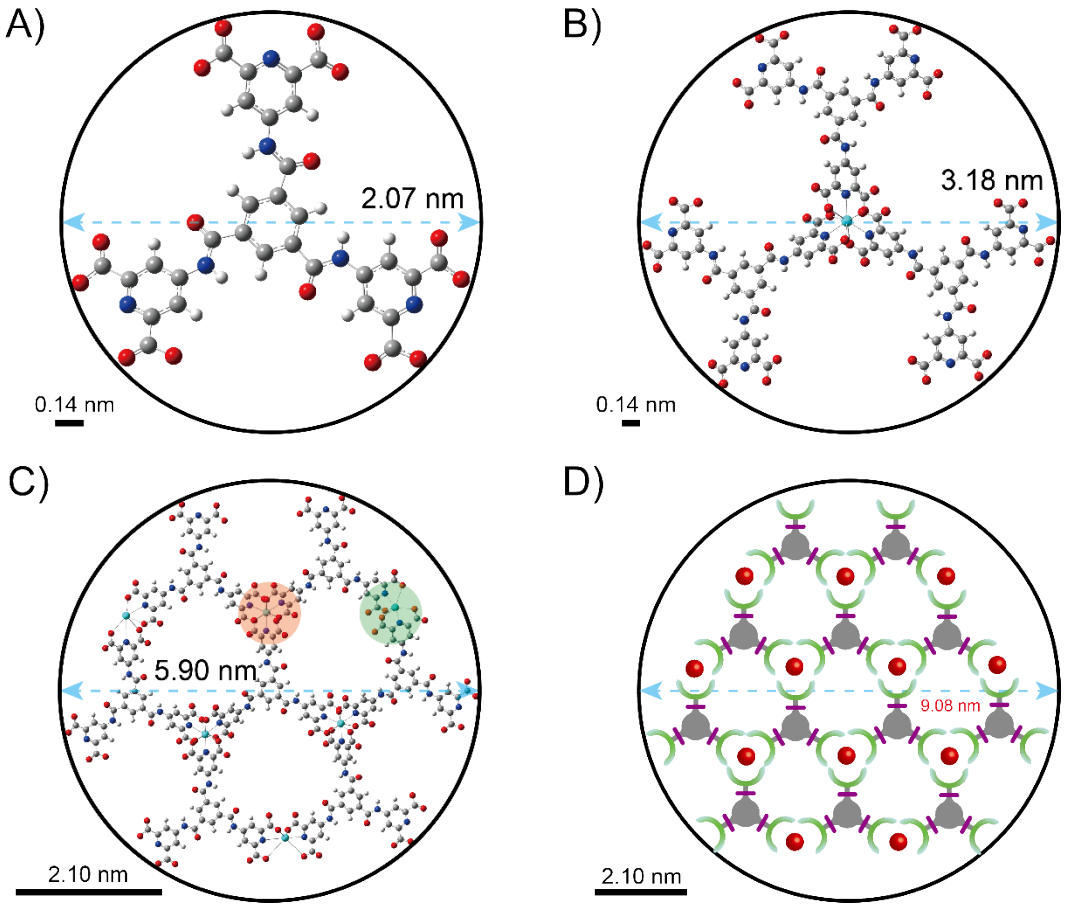

Figure S4. A) The single ligand, 2.07 nm. B) The Eu^{3+}-$(L_3)_3$ complex, 3.18 nm. C) The $Eu^{3+}{}_6$-$(L_3)_7$ complex, 5.90 nm (in the red circle: fully coordinated Eu^{3+}, in the green circle: incomplete coordinated Eu^{3+}). D) The $Eu^{3+}{}_{12}$-$(L_3)_{12}$ complex, 9.08 nm.

The L_3 itself and several metal-ligand clusters were studied by density functional theory (DFT), using the Gaussian 09 program package.[5] The structures were fully optimized by using B3LYP-D3 functions in combination with the def2-SVP basis and the SMD continuum solvent model.[6-9] The complexes $Eu^{3+}{}_6$-$(L_3)_7$ was optimized with GFN-XTB, followed by re-optimization using the Gaussian 09 program. The diameter was measured as that of the smallest circle in which the entire structure could be fitted. The results are shown in Figure S4.

For the single molecule L_3, its size is 2.07 nm; the diameter of Eu^{3+}-$(L_3)_3$ is 3.18 nm; the diameter of $Eu^{3+}{}_6$-$(L_3)_7$ complex is 5.90 nm. Further expanding the cluster to $Eu^{3+}{}_{12}$-$(L_3)_{12}$ complex (Figure S4D) is inapplicable (although it fits the optimal metal/ligand ratio: 1/1). This is because i) there is only 18 sites for combining H_2O molecules, which does not match the $q_{average}$; ii) the model cannot be optimized by GFN-XTB for its large number of atoms and crowding spatial structure; iii) the size for proposed $Eu^{3+}{}_{12}$-$(L_3)_{12}$ complex is measured as 9.08 nm, which is smaller than the size of fiber observed from TEM images. Thus, we speculate that the $Eu^{3+}{}_9$-$(L_3)_{10}$ complex (Figure S3D) is the most representative radial structure for the Eu^{3+}-L_3 fiber.

7. Confirmation of hydrogen bonds

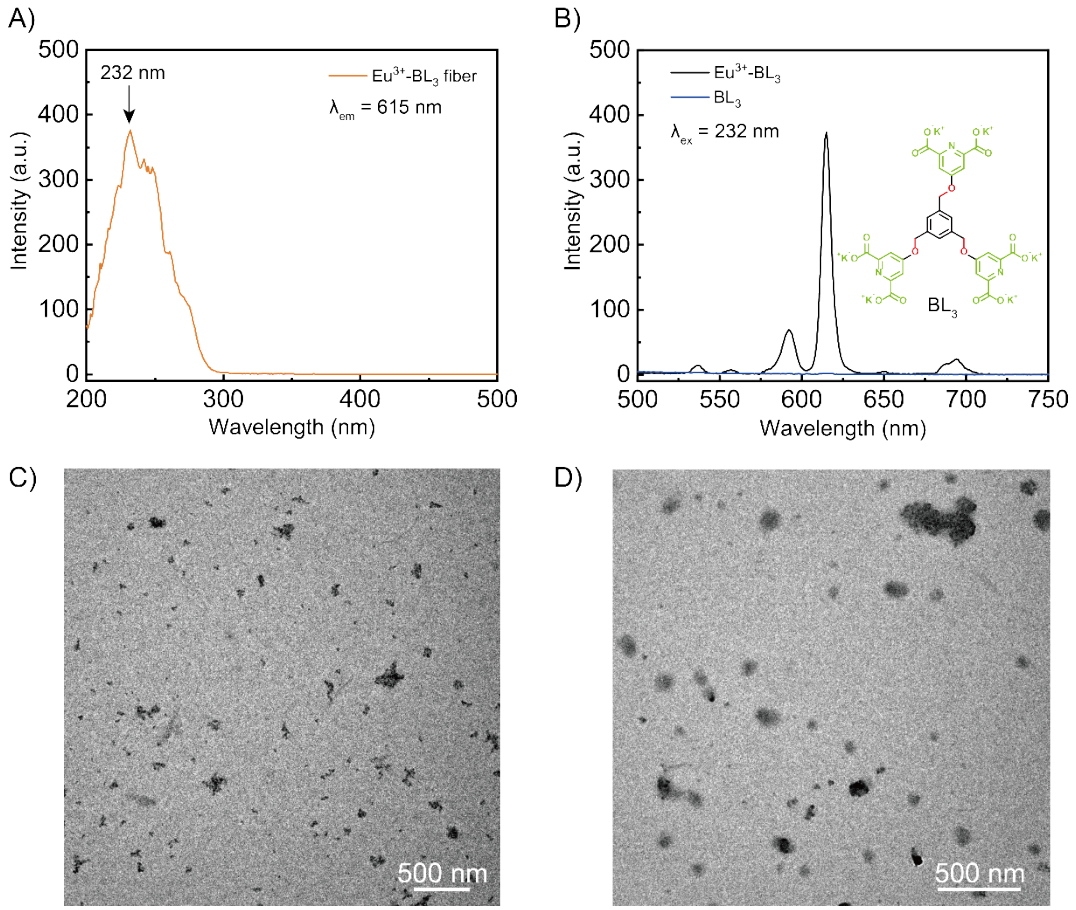

Figure S5. A) Luminescence excitation spectra of Eu^{3+}-BL_3 assemblies taken at emission wavelength λ_{em} = 615 nm. B) Fluorescence emission (λ_{ex} = 232 nm) of BL_3 in the absence of Eu^{3+} ions (blue line), in the presence of Eu^{3+} ions at Eu^{3+}/BL_3 = 1/1 (black line). The chemical structure of BL_3 (Benzene-DPA_3) was inserted in the figure. C) Aggregates formed by Eu^{3+}-BL_3 at Eu^{3+}/BL_3 = 1/1. D) Spherical nanoparticles formed in an Eu^{3+}-L_3 (Eu^{3+}/L_3 = 1/1) solution in the presence of 1 M urea.

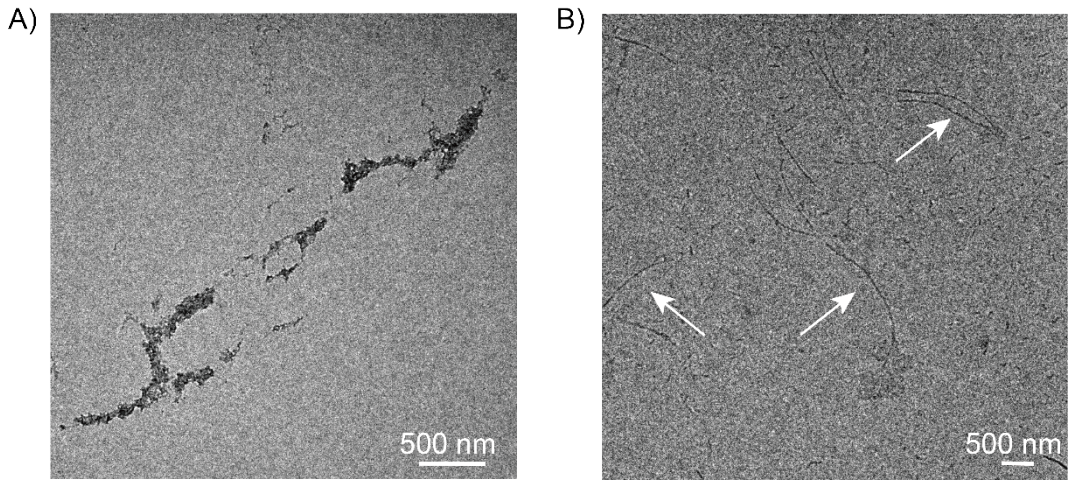

Figure S6. TEM images of Eu^{3+}-L_3 samples at in A) pure water and B) THF/H_2O (v/v = 25/75, white arrows).

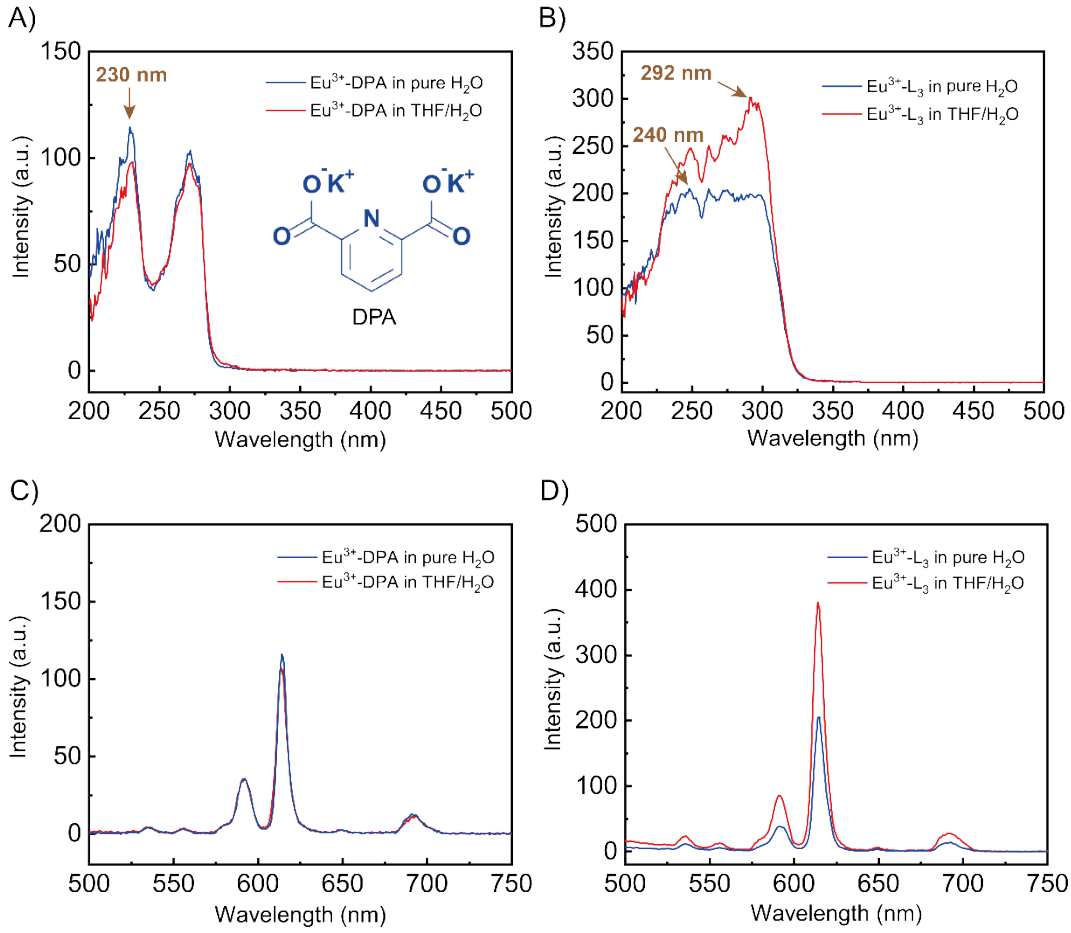

Figure S7. Luminescence excitation spectra of A) Eu^{3+}-DPA and B) Eu^{3+}-L_3 assemblies in pure H_2O or THF/H_2O (v/v = 50/50) taken at emission wavelength

λ_{em} = 615 nm. C) Luminescence emission (λ_{ex} = 230 nm) of Eu^{3+}-DPA assemblies in pure H_2O or THF/H_2O (v/v = 50/50). D) Luminescence emission of Eu^{3+}-L_3 assemblies in pure H_2O (λ_{ex} = 240 nm) or THF/H_2O (v/v = 50/50) (λ_{ex} = 292 nm).

8. Light scattering intensities and TEM images of binary system

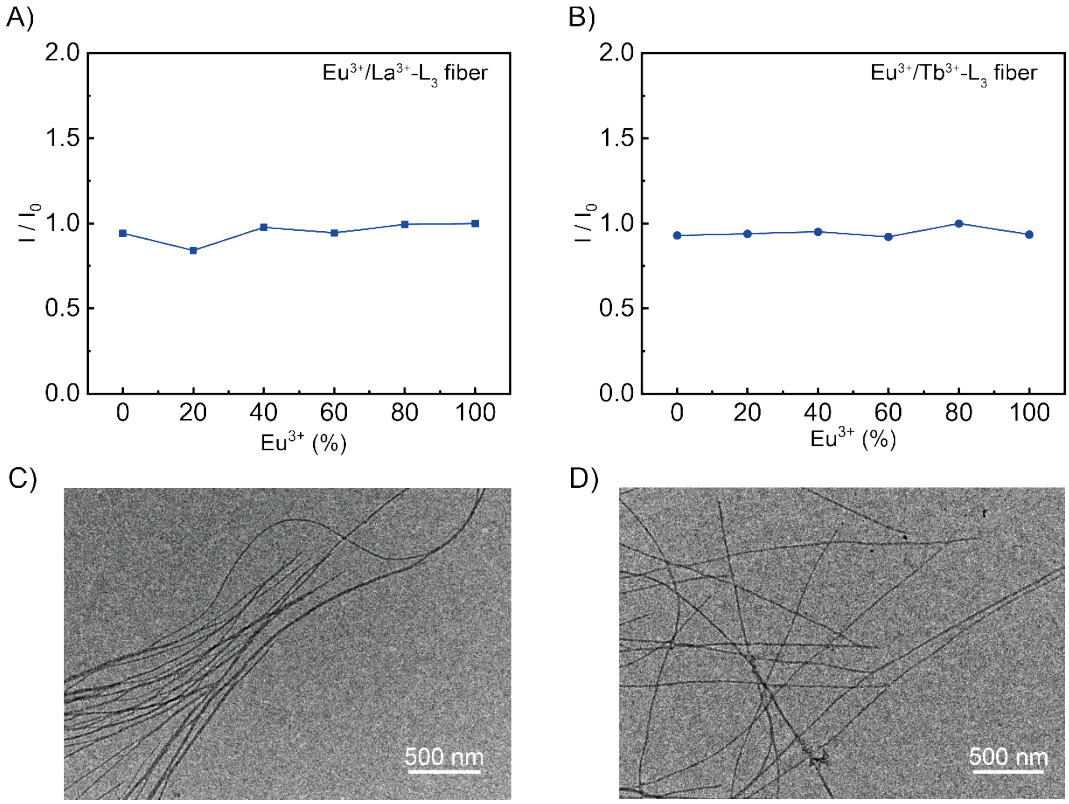

Figure S8. Light scattering intensity of A) Eu^{3+}/La^{3+}-L_3 fibers and B) Eu^{3+}/Tb^{3+}-L_3 fibers at different metal mixing ratios, defined as Eu^{3+}%. C) Fibers formed by Eu^{3+}/La^{3+}-L_3 at Eu^{3+}% = 60%. D) Fibers formed by Eu^{3+}/Tb^{3+}-L_3 at Eu^{3+}% = 60%.

9. Light scattering intensity and TEM image of ternary system

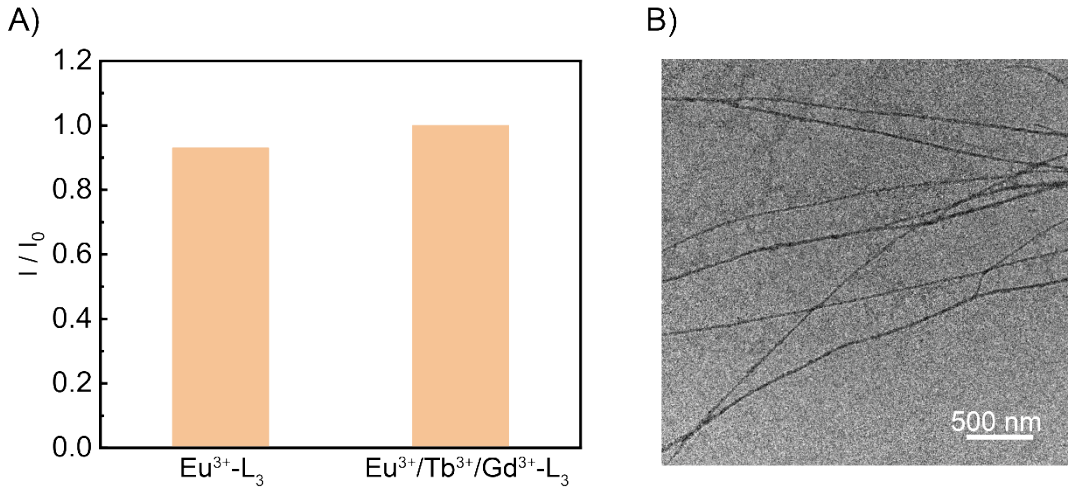

Figure S9. A) Light scattering intensity of $Eu^{3+}/Tb^{3+}/Gd^{3+}$-L_3 ($Eu^{3+}/Tb^{3+}/Gd^{3+}$ = 1/1/1) and Eu^{3+}-L_3 fibers. B) Fibers formed by $Eu^{3+}/Tb^{3+}/Gd^{3+}$-L_3 at $Eu^{3+}/Tb^{3+}/Gd^{3+}$ = 1/1/1.

References

1. B. Wu, L. Liu, L. Zhou, J. R. Magana, M. M. R. M. Hendrix, J. Wang, C. Li, P. Ding, Y. Wang, X. Guo, I. K. Voets, M. A. Cohen Stuart and J. Wang, *J. Colloid Interface Sci.* 2022, **608**, 1297-1307.
2. J. H. Wang, J. Y. Wang, P. Ding, W. J. Zhou, Y. H. Li, M. Drechsler, X. H. Guo and M. A. C. Stuart, *Angew. Chem., Int. Ed.* 2018, **57**, 12680-12684.
3. L. Xu, Y. Jing, L. Feng, Z. Xian, Y. Yan, Z. Liu, J. Huang, *Phys. Chem. Chem. Phys.* 2013, **15**, 16641-16647.
4. Y. Nakano, T. Hirose, P. J. M. Stals, E. W. Meijer and A. R. A. Palmans, Chem. Sci., 2012, **3**, 148-155.
5. Gaussian 09, Revision E.01, M. J. Frisch, G. W. Trucks, H. B. Schlegel, G. E.Scuseria, M. A. Robb, J. R. Cheeseman, G. Scalma-ni, V. Barone, B. Mennucci, G. A. Petersson, H. Nakatsuji, M. Cari-cato, X. Li, H. P. Hratchian,A. F. Izmaylov, J. Bloino, G. Zheng, J. L. Sonnenberg, M. Hada, M. Ehara,K. Toyota, R. Fukuda, J. Ha-segawa, M. Ishida, T. Nakajima, Y. Honda, O.Kitao, H. Nakai, T. Vreven, J. A. Montgomery, Jr., J. E. Peralta, F. Ogliaro, M. Bearpark, J. J. Heyd, E. Brothers, K. N. Kudin, V. N. Staroverov, R. Kobayashi, J. Normand, K. Raghavachari, A. Rendell, J. C. Bu-rant, S. S. Iyengar, J. Tomasi, M. Cossi, N. Rega, J. M. Millam, M. Klene, J. E. Knox, J. B.Cross, V. Bakken, C. Adamo, J.

Jaramillo, R. Gomperts, R. E. Stratmann,O. Yazyev, A. J. Austin, R. Cammi, C. Pomelli, J. W. Ochterski, R. L. Martin,K. Morokuma, V. G. Zakrzewski, G. A. Voth, P. Salvador, J. J. Dannenberg, S. Dapprich, A. D. Daniels, Farkas, J. B. Foresman, J. V. Ortiz, J. Cioslowski, D. J. Fox, Gaussian. Gaussian, Inc., Wallingford, CT, 2009**.**

6. C. Lee, W. Yang and R. G. Parr, *Phys. Rev. B* 1988, **37**, 785-789.
7. A. D. Becke, *Phys. Rev. A* 1988, **38**, 3098-3100.
8. R. F. Ribeiro, A. V. Marenich, C. J. Cramer and D. G. Truhlar, *J. Phys. Chem. B* 2011, **115**, 14556-14562.
9. S. Grimme, *Chem.-Eur. J.* 2012, **18**, 9955-996.